Differential isotropic model of ferromagnetic hysteresis

Jan Pytlík, Jiří Luňáček, and Ondřej Životský
VŠB–Technical University of Ostrava, 17. listopadu 2172/15, 708 00 Ostrava-Poruba, Czech Republic

(Received 30 March 2023; accepted 5 September 2023; published 15 September 2023)

This paper presents an alternative isotropic model of magnetization curves in ferromagnetic materials. It is based on the well-known Jiles-Atherton model, but significantly modifies its assumptions to be consistent with fundamental physical principles. As a result, the number of model parameters has been reduced to four. The differential model couples the volume energy density of the sample with the external magnetic field and includes the process of rigid and flexible overcoming of the pinning sites in the law of energy density conservation. The magnetic moment magnitude is connected with coherent regions called magnetic clusters, which are smaller than magnetic domains. The commonly used concept of anhysteretic magnetization, based on the Langevin function, is modified by a parameter β, which represents the average mutual interaction among magnetic clusters. The model was successfully tested on two isotropic materials: amorphous $Fe_{77.5}Si_{7.5}B_{15}$ alloy and powdered magnetite. The main advantages compared with previous models are the simpler model equation and a much more convenient numerical and fitting procedure.

DOI: 10.1103/PhysRevB.108.104414

I. INTRODUCTION

Scientists have been trying to explain and describe ferromagnetic hysteresis for more than 80 years. Over the decades, numerous approaches have evolved. Micromagnetic methods are used to determine minimum energy of a system in order to find the orientation of magnetic moments; these methods are limited to a small scale. The other extreme is to fit a measured curve with no physical background. Between these two approaches lies an intermediate solution—a global estimation of magnetic behavior based on the methods of statistical physics, modulated by certain microstructural assumptions [1]. The oldest generally known and widely used models include the Preisach model [2] and the Stoner-Wohlfarth model [3]. Both of these models were modified and further developed during the following years, e.g., Refs. [4–7]. In the second half of the 1980s, another model was proposed by Jiles and Atherton [8,9]; it was based on Weiss's original ideas about the magnetic domains and effective magnetic field inside a ferromagnetic material, and it used the key concept, anhysteretic magnetization, based on the modified Langevin function. Later, Harrison introduced a slightly different concept for ferromagnetic hysteresis, with a new dimensionless quantity called the domain coefficient [10]. All these models use different approximations, and so are suitable for different materials and applications [1].

In this paper, our attention is focused on the approach used by Jiles and Atherton and by Venkataraman. Three main forms of the isotropic Jiles-Atherton model can be found in the literature [11]. We designate the previous models by Jiles and Atherton JA1986 [8] and JA1992 [9] and the model by Venkataraman V1998 [12]. All these models have been used for a long time and give adequate results. However, the existence of three forms of the model, as well as recent investigations [11,13], suggest that models are not entirely satisfactory.

The use of the term anhysteretic magnetization (modified Langevin function) is ambiguous in the literature. This function is determined by three parameters: saturation magnetization M_s, magnetic moment size (implicitly given by model parameter a), and interaction coefficient α. It was suggested in Ref. [8] that the magnetic moment size is given by the average domain size. A simple estimation from the fitted data leads to a magnetic moment size $\approx 10^4$–10^6 of Bohr magnetons, which is about five orders higher than atomic magnetic moments and also about seven orders lower than the magnetic moment of the domain [14]. The interaction coefficient α is usually treated as an "interdomain coupling" coefficient [8], while some authors [10,12] claim it to be a "Weiss exchange coefficient." Again, there is a large difference in the value of this parameter between these two approaches.

In previous models [8,9,12], the influence of the effective magnetic field is included twice in the energy density equation—this corresponds to the interaction of the magnetic moment with itself. Moreover, the domain wall flexibility was described by parameter c, though this parameter was not unequivocally defined. The only derivation presented in Ref. [8] is valid solely for small domain wall displacements; this is definitely not valid near the material saturation point.

These discrepancies led us to propose another differential isotropic model of ferromagnetic hysteresis (DIMFH). In this model, the transition from the paramagnetic Langevin function to ferromagnetic Langevin function is achieved via a magnetic cluster assumption. The unclear interaction

coefficient α is replaced by a defined interaction coefficient β. The double effect of the effective field is removed, which leads to a more stable model equation solution and the coefficient β obtains a different meaning. It is shown that the rigid and flexible overcoming of pinning sites is for DIMFH indistinguishable (and should be even for the previous models) from major curve fitting.

II. MODEL DERIVATION

The differential isotropic model of ferromagnetic hysteresis presented here is based on the following ideas:

(1) The exchange interaction of quantum-mechanical origin tends to align atomic magnetic moments, creating the regions of coherent behavior called *magnetic clusters.*

(2) The existence of magnetic clusters leads to the definition of parameter β as the average mutual interaction among clusters. Magnetic domains can be formed by magnetic clusters.

(3) Energy volume density in a sample is given by the external magnetic field H. We claim that there is no physical reason to replace the external field with the effective field H_e as was suggested in Refs. [8,9].

(4) The general problem with domain wall flexibility parameter c is that it is not present in the energy density balance equation. This inconsistency leads us to propose a different parameter definition.

(5) We suppose that magnetic clusters are responsible for the ferromagnetic behavior of the material, and we also expect that their interaction with the pinning sites is responsible for hysteresis (similarly as in Ref. [8]). We use a similar approach to Ref. [8]; however, our definition of the hysteresis coefficient is different.

A. Anhysteretic magnetization

The anhysteretic magnetization curve can be measured experimentally, however, the measurements are difficult to perform [15]. Nevertheless, the anhysteretic magnetization curve is a convenient concept which is frequently used as the basis for models of ferromagnetic hysteresis [8,10].

The functions suitable for anhysteretic magnetization function must have a sigmoidlike shape—odd, nondecreasing functions, zero for zero field, and "converging" to $+M_s$ for a strong positive field and $-M_s$ for a strong field of opposite direction, where M_s is the saturation magnetization. There are a number of functions which meet these conditions [15]. In this paper, we focus only on anhysteretic magnetization based on the Langevin function [8,9].

The Langevin function is derived by methods of classical statistical physics for a set of continuously distributed, mutually noninteracting magnetic moments. This approach was originally used for paramagnetic materials, and some corrections must be performed for ferromagnetic materials.

We focus solely on the isotropic case, so anisotropy energy is not considered. Two significant contributions to energy spectra remain: a classical dipole-dipole interaction and exchange interaction with a quantum-mechanical origin [16]. The exchange interaction aligns atomic magnetic moments to the same direction and is far stronger than the dipole interaction. This leads to the existence of regions consisting of aligned magnetic moments.

The mutual interaction among these regions is classical. Clusters are separated by a transitional region, similar to the domain walls [16]. The exchange interaction is the same on both sides of this transition; there is no significant influence on cluster orientation from the exchange interaction.

The conclusion is that the exchange interaction binds atomic magnetic moments together, resulting in a larger *magnetic cluster* with magnetic moment $\mathbf{m}$, where all atomic moments act collectively.

The average interaction among clusters is more difficult to describe. We suppose that the interaction is proportional to the state of saturation, described by the normalized parameter $f \equiv M/M_s$, where M is the magnitude of magnetization. Since M_s is constant, we can determine the angular dependence of the energy,

$$E_m = -\mu_0 \mathbf{m} \cdot (\mathbf{H} + \beta \mathbf{M}), \tag{1}$$

where $\mathbf{H}$ is the external magnetic field, $\mathbf{M}$ is the magnetization, and μ_0 is the vacuum permeability. Parameter β describes the average mutual interaction between magnetic clusters. Both positive and negative values are allowed. In the case of isotropic material, this parameter is close to zero. We also define parameter a, which originates from the Langevin function [16]

$$a \equiv \frac{k_B T}{\mu_0 m}, \tag{2}$$

where k_B is the Boltzmann constant and T is the thermodynamic temperature. The average value of the magnetic cluster moment m is given by the temperature. This dependence is the subject of further investigation. Using Eq. (1), we can express the anhysteretic magnetization M_{an} using the modified Langevin function

$$\begin{aligned} M_{an} &= M_s \left[\coth\left(\frac{H+\beta M)}{a}\right) - \frac{a}{H+\beta M}\right] \\ &= M_s \mathcal{L}\left(\frac{H+\beta M}{a}\right). \end{aligned} \tag{3}$$

This derivation can be done only if $\frac{\partial M}{\partial H} \to 0$, otherwise Eq. (3) leads to a differential equation with no solution suitable for anhysteretic magnetization.

It should be noted that the magnitude of the cluster magnetic moment is large enough so that no quantum effects are significant and all the assumptions of the derivation of the Langevin function are fulfilled. To demonstrate the influence of the magnetic moment magnitude, Fig. 1 presents the ordinary Langevin function [Eq. (3) with $\beta = 0$] for three magnetic moment magnitudes: the ferromagnetic domain $m = 1.10^{13}\mu_B$ ($a \cong 3.55\times10^{-5}$ A/m) [14], the magnetic cluster $m = 1.10^{5}\mu_B$ ($a \cong 3.55\times10^{3}$ A/m), and the atomic magnetic moment $m = 2\mu_B$ ($a \cong 1.78\times10^{8}$ A/m), where μ_B is the Bohr magneton.

From Fig. 1 is obvious that the magnetic moment magnitude m has a critical impact on the anhysteretic magnetization curve slope and shape. Hysteretic curves inherit their slope from the anhysteretic curve. Only the intermediate solution

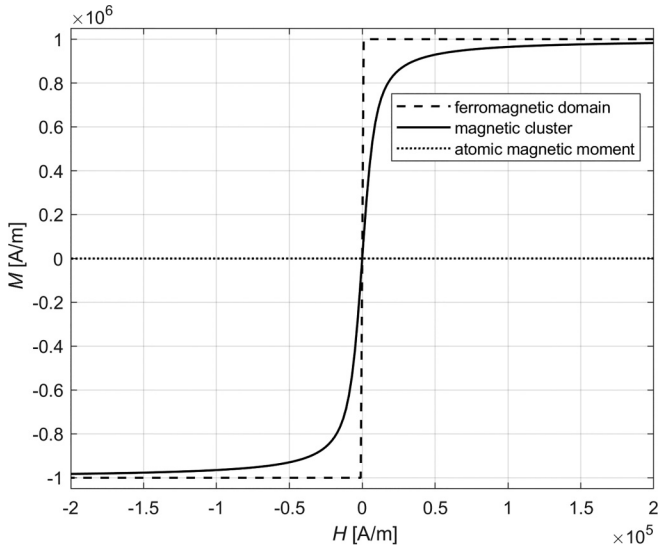

FIG. 1. Influence of parameter a on the anhysteretic Langevin magnetization curve shape. Curve simulations were done by solving Eq. (3) with $\beta = 0$ and $M_s = 10^6$ A/m. The values of a correspond to the ferromagnetic domain magnetic moment $a \cong 3.55\times10^{-5}$ A/m, the cluster magnetic moment $a \cong 3.55\times10^{3}$ A/m, and the atomic magnetic moment $a \cong 1.78\times10^{8}$ A/m.

using the magnetic cluster assumption corresponds to the measured magnetization curve slopes, as shown later.

B. The pinning process

During the magnetization process, the orientation of the magnetic moments of the magnetic clusters is changed. So far, we have supposed that nothing other than temperature excitation prevents cluster magnetic moments from aligning to the external magnetic field. However, in a real material, pinning sites are present [8]. We assume that pinning sites are local stress centers, which are caused by different mechanisms (dislocations, grain boundaries, etc.) and interact with magnetic moments through the magnetoelastic effect. The energy dissipated by overcoming the pinning site (PS) is [8]

$$E_{\mathrm{PS}} = \frac{\epsilon_\pi}{2}(1-\cos\varphi), \tag{4}$$

where ϵ_π is the maximum energy dissipated by the PS and φ is the angle between the direction of the magnetization (given by the external magnetic field direction) and the intrinsic cluster magnetic moment direction (given by the PS orientation).

We assume a homogeneous distribution of pinning sites, introducing PS volume density ρ_{PS}, and we substitute ϵ_π by its average value $\langle\epsilon_\pi\rangle$. Then, the energy dissipated by pinning can be expressed as

$$E_{\mathrm{pin}} = \int E_{\mathrm{PS}}\rho_{\mathrm{PS}}\, dV_{\mathrm{CR}}, \tag{5}$$

where the element dV_{CR} is the volume where the cluster orientation has been changed. This volume is clearly related to the change in magnetization.

For simplicity, we suppose that the part of the material with volume V consists of two large areas with the same orientation of magnetic moments with volumes V_1 and V_2. The atomic

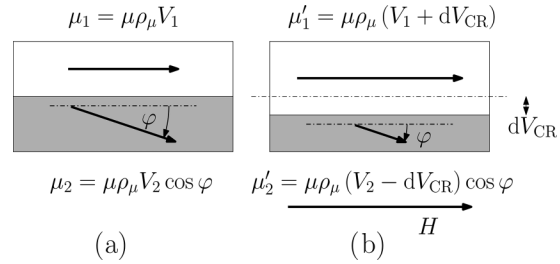

FIG. 2. Part of the material with two areas with the same orientation of magnetic moments (a) in a demagnetized state, and (b) with an applied external magnetic field. The volume of the region with the orientation parallel to the external magnetic field is increased.

magnetic moment of the material is μ and the density of atomic magnetic moments is ρ_μ. If an external magnetic field H is applied, the volume of the region with the orientation parallel to the external magnetic field is increased by dV_{CR}. In an ideal case, $\mu\rho_\mu = M_s$.

Using Fig. 2, we can write

$$\begin{aligned} dM &= \frac{\mu_1' + \mu_2'}{V} - \frac{\mu_1 + \mu_2}{V} \\ &= \frac{1}{V}\mu\rho_\mu(1-\cos\varphi)dV_{\mathrm{CR}}. \end{aligned} \tag{6}$$

Using Eqs. (4)–(6), we can write the final statement for energy density dissipated during the magnetization process as

$$w_{\mathrm{pin}} = \int \frac{\langle\epsilon_\pi\rangle}{2}\frac{\rho_{\mathrm{PS}}}{\mu\rho_\mu}dM = k\int \frac{dM}{dH}\,dH, \tag{7}$$

where the coefficient $k = \frac{\langle\epsilon_\pi\rangle}{2}\frac{\rho_{\mathrm{PS}}}{\mu\rho_\mu}$ describes pinning. This derivation of parameter k *differs* from that presented in Ref. [8].

The possible flexibility of the cluster structure can influence the interaction of clusters with pinning sites. In Ref. [8], the authors derived a relation describing domain wall flexibility, where the energy density "saved" from pinning is proportional to the difference between anhysteretic and total magnetization,

$$w_{\mathrm{rev}} \propto c'(M_{\mathrm{an}} - M). \tag{8}$$

Coefficient c' has a positive value. This relation is only valid for small domain wall bulging. In later papers [9,12], coefficient c' is replaced by coefficient $c \in \langle 0, 1\rangle$, which describes the reduction of energy dissipated on the pinning sites, with no description of the mechanism.

A major problem with both coefficients is that they are not present in the energy density balance equation, and therefore they have no influence on the energy equilibrium. We also believe that the pinning process is bound to the magnetic clusters rather than domain walls.

The reduction of energy density dissipation w_{rev} on a PS can be described by

$$w_{\mathrm{rev}} \leqslant w_{\mathrm{pin}} \rightarrow w_{\mathrm{rev}} = c w_{\mathrm{pin}}. \tag{9}$$

It is obvious from Eqs. (9) and (7) that coefficients k and c are bound together. Using Eq. (8) instead of Eq. (9) leads to a comparable result. The effect of the flexible pinning process

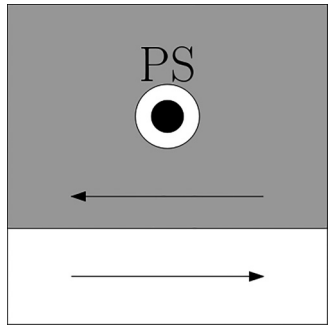

FIG. 3. Schematic proposition of a mechanism which reduces energy dissipation on PS via flexible cluster structure behavior. The expanding oriented region (gray) overcame the pinning site; however, a small region around PS remained unchanged, so no dissipation via PS breaking is present.

will be reflected in the magnetization curve as a reduction in the number of PSs. In the case of a strong pinning effect, even inflexible bulging is more efficient than breaking PS. This would lead to PS evasion, with a small region remaining unchanged, as shown schematically in Fig. 3. This possibility is the subject of further investigation.

We also assume that the coefficient c is a function of the state of magnetization $f \equiv \frac{M}{M_s}$. For simplicity, we suppose in the first approximation that the coefficient c is constant. If so, it is impossible to distinguish the influence of coefficients k and c on the curve shape from the measured major hysteresis loop.

C. Model equation derivation

Energy density can be expressed from the area below the magnetization curve as

$$w = \mu_0 \int M\, dH = \mu_0 \int M(H + \beta M) dH. \tag{10}$$

This relation differs from $w = \mu_0 \int M\, dH_e$, used in previous papers [8,9,12], because only the external magnetic field H is applied to the material. The effective magnetic field in the material is different [see Eq. (1)], and it is defined differently, by the parameter β which characterizes the average mutual interaction among clusters.

Now we can write the final energy density balance equation using Eqs. (3), (7), (9), and (10) as

$$w = w_{\text{an}} - w_{\text{pin}} + w_{\text{rev}},$$

$$\mu_0 \int M\, dH = \mu_0 \int M_{\text{an}}\, dH - k \int \frac{dM}{dH}\, dH + ck \int \frac{dM}{dH}\, dH,$$

$$M = M_{\text{an}} - \delta \frac{k}{\mu_0}(1-c)\frac{dM}{dH}, \tag{11}$$

where δ represents the fact that the pinning always acts against the external magnetic field. We define the parameter $h \equiv \frac{k}{\mu_0}(1-c)$. If $h = 0$, Eq. (11) is reduced to the anhysteretic case $M = M_{\text{an}}$. In the case of a hysteresis curve ($h \neq 0$), we can write the final equation for the differential model of ferromagnetic hysteresis (DIMFH) using Eqs. (3) and (11) as

$$\frac{dM}{dH} = \frac{M_{\text{an}} - M}{\delta h} = \frac{M_s \mathcal{L}\left(\frac{H+\beta M}{a}\right) - M}{\delta h}. \tag{12}$$

Compared to previous models [8,9,12], this equation has a much simpler form and uses one fewer parameter.

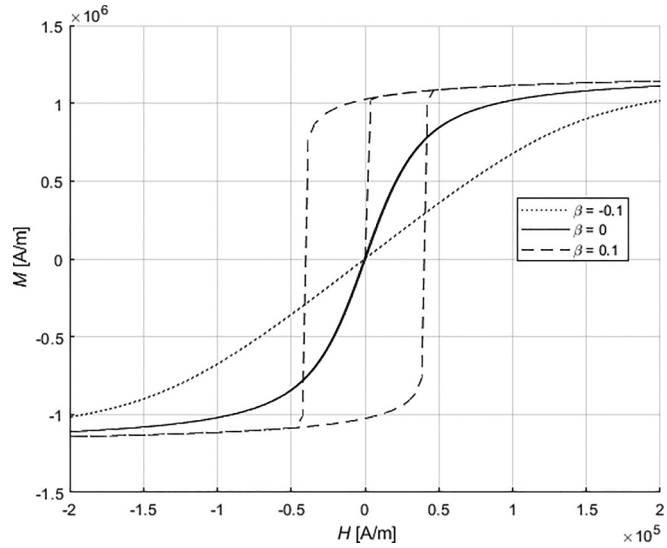

FIG. 4. Influence of parameter β on magnetization curve shape. Curve simulations were done by solving Eq. (12) with the Runge-Kutta fourth-order solver, on 25 000 points of a simulated magnetic field. The parameters were $M_s = 1.2\times10^6$ A/m, $a = 15\,000$ A/m, and $h = 500$ A/m.

D. Influence of β

In models JA1986, JA1992 and V1998, low values of parameter α have a low impact on the magnetization curve shape, whereas larger values of α lead to curve instability and the "artificial limit" $\frac{dM}{dH} \to -\frac{1}{\alpha}$.

The DIMFH uses parameter β and appears to be more stable and without an artificial limit. Figure 4 shows the influence of parameter β on the magnetization curve. Negative β decreases the slope of the curve, while positive β leads to a significant increase in coercivity.

The solution of Eq. (12) is found using the well-known Runge-Kutta fourth-order solver with the initial condition $M(H = 0) = 0$. This initial condition is the same for all curve simulations. The alternation of δ is performed in the curve turning points.

III. EXPERIMENTAL CURVE FITTING AND COMPARISON OF MODELS

The applicability of the proposed model was tested on two types of experimental samples: an amorphous $Fe_{77.5}Si_{7.5}B_{15}$ alloy [17] prepared in the form of a 20-μm-thick ribbon using planar flow casting technology, and homogenized magnetite powder (Precheza Prerov, Czech Republic) with an average gain size of approximately 1 μm. Both samples meet the condition of isotropic materials well. The magnetization curves of ribbon and powder samples at room temperature were fitted

TABLE I. Comparison of the fitted parameters of the DIMFH with models based on the Jiles-Atherton approach. The room-temperature magnetization curves were measured on the $Fe_{77.5}Si_{7.5}B_{15}$ ribbon (321 measured points) and powder magnetite (945 measured points).

Model	M_s (A/m)	a (A/m)	k (A/m)	α (−)	c (−)	c' (−)	h (A/m)	β (−)	S (A/m)	r^2 (−)
Amorphous $Fe_{77.5}Si_{7.5}B_{15}$ ribbon										
JA1986	1373103	2366	297.7	0.000384		133.9			6115	0.999979
JA1992	1372000	2309	123.9	0.000067	0.551				7448	0.999969
V1998	1372237	2337	126.0	0.000162	0.554				7142	0.999971
DIMFH	1374714	2602					93.0	0.001071	4834	0.999987
Magnetite powder										
JA1986	62813	30831	15552	0.07319		0			1246	0.99911
JA1992	63946	38568	17162	0.48234	0.1719				1178	0.99920
V1998	63942	38555	16467	0.47980	0.0467				1175	0.99921
DIMFH	62964	32258					14391	0.1612	1123	0.99928

by proposed DIMFH as well as by other models based on the Jiles-Atherton approach [8,9,12]. The results are summarized in Table I. The quality of the fit is controlled by parameter S, defined as

$$S = \sqrt{\frac{\sum_i^N (M_i - M_{\text{expt},i})^2}{N}}, \tag{13}$$

where $M_{\text{expt},i}$ are measured curve points, N is the number of measured curve points, and M_i are simulated points corresponding to $M_{\text{expt},i}$.

To express the relative accuracy of the fit, the r^2 coefficient is implemented,

$$r^2 = 1 - \frac{\sum_i^N (M_i - M_{\text{expt},i})^2}{\sum_i^N (\overline{M}_{\text{expt}} - M_{\text{expt},i})^2}, \tag{14}$$

where $\overline{M}_{\text{expt}}$ is the arithmetic average of the measured magnetization points.

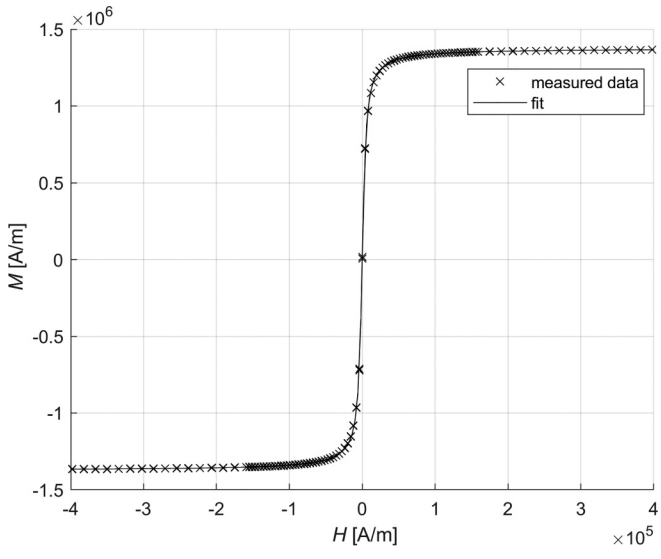

FIG. 5. The measured (crosses) and fitted (solid line) magnetization curve of an amorphous $Fe_{77.5}Si_{7.5}B_{15}$ ribbon using the DIMFH. The measured curve consists of 321 points and its simulation was done by the Runge-Kutta fourth-order solver. To improve the fit accuracy $n = 86$ interpolated points were inserted between two measured points. The resulting parameters are summarized in Table I.

To maintain accuracy in the simulated curve, n additional magnetic field values are inserted between every two measured magnetic field values. The number n increases until the simulated curve is considered stable. By fitting a series of curves, the following stability criterion was found: The average coercive field difference between two adjacent values of n must be lower than 0.5 A/m.

Figure 5 shows the measured room-temperature magnetization curve of the $Fe_{77.5}Si_{7.5}B_{15}$ ribbon and the corresponding fitted curve using the DIMFH. Comparing the DIMFH with other models (see the upper part of Table I), the parameters M_s and a are very similar, as is also the accuracy of the fit. From the fitted values of parameter a and from Eq. (3), it is possible to calculate the number of Bohr magnetons corresponding to magnetic moment m. The result is $\approx 10^4$–10^6, which is about five orders higher than the atomic magnetic moments and also about seven orders lower than the magnetic moment of the ferromagnetic domain. This supports the proposed cluster mechanism. We can conclude that the fitted values of parameter a were determined correctly in the previous models [8,9,12], however, the physical interpretation of m does not correspond to the magnetic domain moment. Moreover, magnetic domains do not meet the assumptions of the Langevin function. The mentioned discrepancy in the value of magnetic moment m was not identified by any of the authors.

The fitting program was written in the MATLAB environment, and the code is freely available in the Supplemental Material [18]. The fitting speed is very good. On a standard desktop personal computer (used parameters: 64-bit MATLAB, Windows 8.1, AMD Radeon R7 4×3.5 GHz, RAM 8 GB), the fitting time of one loop is about 30 s. All fitted parameters (M_s, a, h, β) as per Sec. II have a clear physical meaning. A similarly good agreement between the experimental data and the fit can be observed in the case of the magnetite powder (see the lower part of Table I). Figure 6 shows the measured room-temperature magnetization curve of the magnetite powder and the corresponding fitted curve using the DIMFH.

IV. CONCLUSION

In this paper, we have proposed a differential isotropic model of ferromagnetic hysteresis (DIMFH) that is based on

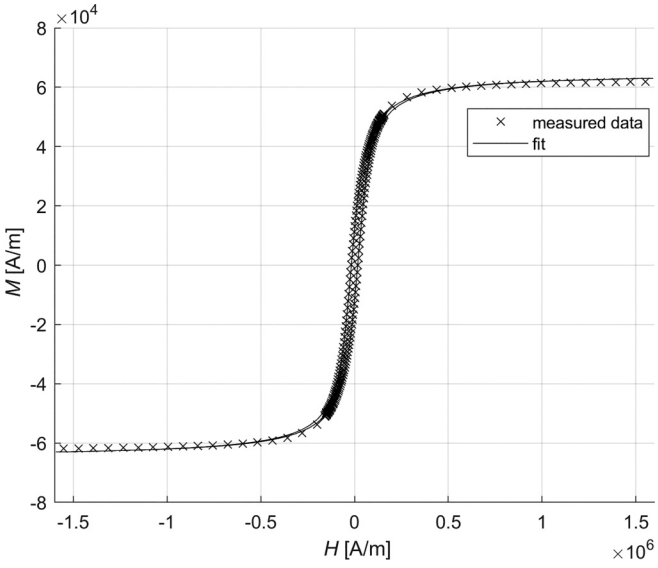

FIG. 6. The measured (crosses) and fitted (solid line) magnetization curve of a powdered magnetite using the DIMFH. The measured curve consists of 945 points and its simulation was done by the Runge-Kutta fourth-order solver. To improve the fit accuracy $n = 29$ interpolated points were inserted between two measured points. The resulting parameters are summarized in Table I.

two assumptions: (1) The energy density [Eq. (10)] forms the energy density balance equation [Eq. (11)]. (2) The ideal anhysteretic curve [Eq. (3)] is modified by overcoming the pinning sites in the material [Eq. (7)].

In this model, ferromagnetic behavior is given by an interaction of nonclassical origin, which results in the formation of magnetic clusters. The average size of the magnetic clusters is included in parameter a, while the mutual average interaction among the clusters is described by parameter β. Both rigid and flexible overcoming of the pinning sites is described by parameter h.

The proposed differential isotropic model of ferromagnetic hysteresis remains in full generality, but in comparison to the previous models it has the following advantages: (1) The model has a far simpler form, as can be seen from the final Eq. (12). (2) Only four model parameters are used (M_s, a, h, and β). (3) Numerical processing and fitting are much more convenient.

Nevertheless, several matters still remain unresolved: (1) An extension of the model to anisotropic materials is currently in preparation. (2) The approach based on the major anhysteretic curve is valid only for the major magnetization curve. To cover minor hysteresis loops, an adjustment to the model needs to be performed. (3) No description exists for the flexible overcoming of the pinning sites near the material saturation point. The dependence of parameter c on the state of magnetization is not yet known. (4) The temperature dependence of saturation magnetization M_s and the average cluster size moment m are not yet solved.

ACKNOWLEDGMENT

This work was funded by the Ministry of Education, Youth and Sports of the Czech Republic under Projects No. SP 2023/036 and No. CZ.02.1.01/0.0/0.0/17_048/0007399.

[1] F. Liorzou, B. Phelps, and D. Atherton, Macroscopic models of magnetization, IEEE Trans. Magn. **36**, 418 (2000).
[2] F. Preisach, Über die magnetische nachwirkung, Z. Phys. **94**, 277 (1935).
[3] E. C. Stoner and E. P. Wohlfarth, A mechanism of magnetic hysteresis in heterogeneous alloys, Philos. Trans. R. Soc. London Ser. A **240**, 599 (1948).
[4] I. Mayergoyz, Mathematical models of hysteresis, IEEE Trans. Magn. **22**, 603 (1986).
[5] H. A. J. Cramer, A moving Preisach vector hysteresis model for magnetic recording media, J. Magn. Magn. Mater. **88**, 194 (1990).
[6] W. Wernsdorfer, E. B. Orozco, B. Bonet, B. Barbara, K. Hasselbach, A. Benoit, D. Mailly, B. Doudin, J. Meier, J. E. Wegrowe, J.-P. Ansermet, N. Demoncy, H. Pascard, A. Loiseau, L. Francois, N. Duxin, and M. P. Pileni, Mesoscopic effects in magnetism: Submicron to nanometer size single particle measurements, J. Appl. Phys. **81**, 5543 (1997).
[7] A. P. Roberts, D. Heslop, X. Zhao, and C. R. Pike, Understanding fine magnetic particle systems through use of first-order reversal curve diagrams, Rev. Geophys. **52**, 557 (2014).
[8] D. C. Jiles and D. Atherton, Theory of ferromagnetic hysteresis, J. Magn. Magn. Mater. **61**, 48 (1986).
[9] D. C. Jiles, J. Thoelke, and M. Devine, Numerical determination of hysteresis parameters for the modeling of magnetic properties using the theory of ferromagnetic hysteresis, IEEE Trans. Magn. **28**, 27 (1992).
[10] R. G. Harrison, A physical model of spin ferromagnetism, IEEE Trans. Magn. **39**, 950 (2003).
[11] R. Szewczyk and P. Cheng, Open source implementation of different variants of Jiles-Atherton model of magnetic hysteresis loops, Acta Phys. Pol. A **133**, 654 (2018).
[12] R. Venkataraman and P. Krishnaprasad, Qualitative analysis of a bulk ferromagnetic hysteresis model, in *Proceedings of the 37th IEEE Conference on Decision and Control* (IEEE, New York, 1998), Vol. 3, pp. 2443–2448.
[13] J. B. Padilha, P. Kuo-Peng, N. Sadowski, J. Leite, and N. Batistela, Restriction in the determination of the Jiles-Atherton hysteresis model parameters, J. Magn. Magn. Mater. **442**, 8 (2017).
[14] D. C. Jiles, *Introduction to Magnetism and Magnetic Materials*, 1st ed. (Springer, Berlin, 1991).
[15] M. Nowicki, R. Szewczyk, and P. Nowak, Experimental verification of isotropic and anisotropic anhysteretic magnetization models, Materials **12**, 1549 (2019).
[16] K. M. Krishnan, *Fundamentals and Applications of Magnetic Materials* (Oxford University Press, Oxford, UK, 2016).

[17] O. Zivotsky, A. Titov, Y. Jiraskova, J. Bursik, J. Kalbacova, D. Janickovic, and P. Svec, Full-scale magnetic, microstructural, and physical properties of bilayered CoSiB/FeSiB ribbons, J. Alloys Compd. **581**, 685 (2013)

[18] See Supplemental Material at http://link.aps.org/supplemental/10.1103/PhysRevB.108.104414 for code made to fit experimental magnetization curve with DIMFH model, using basic MATLAB functions.